NTU Journal of Engineering and Technology (ICSDT2025) special issue
DOI: https://doi.org/10.56286/ntujet.icsdt2025

IRAQI Academic Scientific Journals

P-ISSN: 2788-9971 E-ISSN: 2788-998X
NTU Journal of Engineering and Technology
Available online at: https://journals.ntu.edu.iq/index.php/NTU-JET/index

Classification of Alzheimer's Disease Using a Hybrid Technique Integration Between CNN and Optuna Optimization

Nawzt Sadiq Jaafar Al-Bayati[1, 2], Raid Rafi Omar Al-Nima[3]
[1]Technical Engineering College / Mosul, Northern Technical University, Mosul, Iraq
[2]Vocational Education Department, Directorate of Ninawa Education, Ministry of Education, Mosul, Iraq
[3]Technical Engineering College for Computer and Artificial Intelligence / Mosul, Northern Technical University, Mosul, Iraq
nawzt.sadek@ntu.edu.iq, raidrafi1@gmail.com

Article Informations

Received: 15-03- 2025,
Accepted: 28-04-2025,
Published online: 01-03-2026

Corresponding author:
Name: Nawzt S. J. Al-Bayati
Affiliation: Northern Technical University
Email: nawzt.sadek@ntu.edu.iq

Key Words:
Alzheimer's disease, Convolutional Neural Network, Optuna optimization, classification.

A B S T R A C T

Alzheimer's Disease (AD) is considered one of the most prevalent neurological disorders, primarily affecting elderly people and adversely impacting their brain functions. This disease is characterized by the gradual deterioration of cognitive functions, particularly memory, leading to varying information loss levels, typically classified within the framework of dementia. In this context, Artificial Intelligence (AI) methods, especially Convolutional Neural Networks (CNN) and Optuna optimization, have emerged as effective technique to provide efficient approach (or model) for classifying AD levels. The proposed approach is called the Optuna-CNN (O-CNN). It has the ability to identify the optimal CNN architecture by employing the optimization of Optuna. It is designed to classify AD into four levels (or stages): Mild Dementia (MD), Moderate Dementia (MoD), No Dementia (ND) and Very Mild Dementia (VMD). Two datasets are utilized here: the Best Alzheimer's MRI Dataset (BA-MRI) and the Alzheimer's MRI Dataset (AD-MRI), both are obtained from Kaggle platform. Following extensive training and implementations of the O-CNN method, high classification accuracies 94.79% for the AD-MRI dataset and 99.18% for the BA-MRI dataset are achieved.

1. Introduction

Alzheimer's Disease (AD) is a progressive neurodegenerative disorder that affects nerve cells in the brain and is one of the most common diseases among older age groups of people [1]. The disease causes a decline in memory and cognitive abilities due to the increasing damage of nerve cells. AD is classified as a type of dementia [2]. The brain changes associated with AD cause significant deterioration in the daily life of those affected persons [3]. Symptoms begin with a gradual loss of memory and difficulty remembering recent events, and progress to include forgetting people, places, and dates. Ultimately, patients become unable to perform simple daily tasks. It is also considered a serious disease due to its effect on the gradual deterioration of symptoms over time. The development of this disease is attributed to a complex interaction between biological factors, including endogenous anticholinergic activity, downregulation of the neurotransmitter acetylcholine, and chronic inflammatory processes. These factors work together to accelerate cognitive decline and lead to the accumulation of amyloid plaques in the brain [4], especially during the middle stage of the disease [5][6]. Fig. 1. A comparison of a (a) healthy brain and (b) a brain affected by advanced AD.

AD presents a substantial challenge not only for patients but also for caregivers [7], who experience immense psychological stress due to the constant need for support and care. Therefore, comprehending the levels of AD and its impact on individuals and caregivers is crucial for awareness and treatment efforts.

This study aims to categorize AD into its various levels of: Mild Dementia (MD), Moderate Dementia (MoD), Non-Dementia (ND) and Very Mild Dementia (VMD). Our study contributes in enhancing CNN performance by exploiting the Optuna optimization. The proposed model is named the Optuna-CNN (O-CNN), which can effectively diagnose and classify various AD stages.

The remaining sections of this paper are organized as follows: Section 2 offers a review of the literature, Section 3 explains the proposed O-CNN approach, Section 4 details the two utilized datasets and discusses the experimental outcomes, and Section 5 concludes the paper.

2. Literature Review

A compilation of earlier researches that have investigated the topic of AD can be outlined as follows:

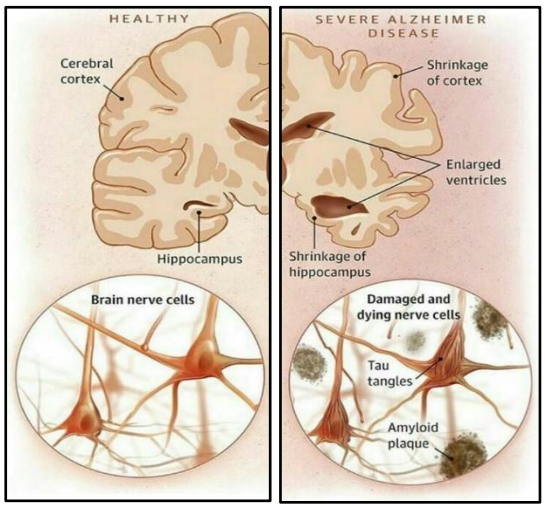

Fig. 1. A comparison of a (a) healthy brain and (b) a brain affected by advanced AD.

In 2013, Vos et al. conducted a study to predict Alzheimer for people with mild and moderate cognitive impairment. Biological and structural indicators, such as Beta-Amyloid (BA) protein, Total Tau (T-Tau) in cerebrospinal fluid, Hippocampal Volume (HCV) and Apolipoprotein E gene, were analyzed. The study included 399 subjects with mild cognitive impairment of dementia and 226 without. The results showed that the indicators significantly improved early diagnosis of Alzheimer [8].

In 2014, Fiscon et al. proposed a computational design for analyzing Electroencephalogram (EEG) signals to support diagnosing AD and MCI. Comprehensive analysis was identified to have broad applications, including basic analysis and time-frequency economic analysis. The dataset used in this study consisted of 100 samples. Various classification methods were employed such as SVM, decision tree and rule-based classifiers. The best accuracy of 90% was achieved by using the decision tree classifier [9].

In 2015, Gorji and Haddadnia introduced a novel method for the early diagnosis of AD based on Pseudo Zernike Moments (PZMs). Discriminative information was extracted from structural MRI images. Two types of artificial neural networks were employed: Pattern Recognition Network (PRN) and Learning Vector Quantization (LVQ) network. ADNI database of 500 images were utilized. The highest accuracy of 95.59% was achieved [10].

In 2016, Jha and Kwon developed a new method for diagnosing AD using Curvelet Transform (CT) and K-Nearest Neighbors (K-NN) techniques. The CT was employed for extracting features from MRI images. Then, Principal Component Analysis (PCA) was applied to reduce dimensionality. After that K-NN along with Artificial Neural Network (ANN) were utilized for classification. MRI data from the Open-Source Imaging Studies Series (OASIS), including 416

individuals aged 18 to 96 years, was utilized. The proposed method achieved a classification accuracy of 89.47% [11].

In 2017, Gulhare and Sharma designed a technique for early detection of AD using a Deep Neural Network (DNN) architecture on brain MRI images. The images were segmented using the Niblack thresholding algorithm and features were extracted from the segmented regions using image processing techniques. A DNN classifier was then exploited to distinguish between normal tissue and AD tissue. The database here was for 150 individuals, 88 women and 62 men, aged between 60 and 96 years where 72 persons were without dementia and 78 persons were with dementia. The accuracy in this study was reached 96.6% [12].

In 2018, Khvostikov et al. constructed a Three-Dimensional (3D) CNN to classify AD using structural MRI and DTI images. Advanced feature extraction techniques such as Gauss-Laguerre Harmonic Functions (GL-CHFs) were applied, which helped to identify ROIs in brain images. The Bag-of-Visual Words (BoVW) model was then used to encode the extracted features. A dataset of 280 samples was employed in this work. An accuracy of 92.5% was achieved in the results [13].

In 2019, Maqsood et al. designed an automated system for early detection and classification of AD using transfer learning techniques. The pre-trained convolutional network of AlexNet was utilized and the last layers were adapted to suit the classification of AD levels. The system was trained and tested on segmented and non-segmented images including Gray Matter (GM), White Matter (WM), and Cerebrospinal Fluid (CF) features. The system performance was evaluated using 382 3D MRI images of OASIS dataset, where a remarkable accuracy of 92.85% was obtained for the classification of non-segmented images [14].

In 2020, Rajak and Shrivastava investigated machine learning techniques to improve early detection and effectively diagnose AD. Such techniques were Logistic Regression (LR), SVM, Decision Tree (DT), Random Forest (RF) and Adaboost, which were aimed to be applied to MRI data and leveraged. The longitudinal OASIS dataset with 373 records and 15 features was used. The highest performances were achieved by the RF and Adaboost algorithm [15].

In 2021, Bi et al. aimed to evaluate the performance and stability of a Deep Metric Learning (DML) algorithm in analyzing MRI images for AD diagnosis. An early diagnosis system was developed using both CNN and DML algorithms, with comparing their performances in classifying MRI images. Processing stages included image correction, bone removal, cross-entropy loss, and measurement loss. It was indicated that the DML algorithm could significantly contribute to the early diagnosis of AD, although increasing the sample size in future studies was suggested to strengthen the results. Data from the ADNI dataset were used, which included a total of 578 samples. 83% accuracy was achieved by this algorithm [16].

In 2022, Sheng et al. developed a technique for predicting AD using brain imaging and genetic data. MRI images were combined with genetic data to improve the performance. Fisher Score (FS) was utilized to reduce the dimensionality of genetic features before they were combined with imaging features. SVM algorithm was applied for classification and cross-validation was exploited to evaluate the overall model, it increased the reliability of the results. A notable accuracy rate of 98% has been secured with this technique [17].

In 2023, Khan et al. suggested transfer learning models of VGG16 and Visual Geometry Group 19 (VGG19) to classify different stages of AD. A tissue segmentation technique was applied to extract GM features from MRI images. The GM was used to fine-tune the pre-trained VGG architecture with freezing features of the ImageNet database. This was accomplished by adding a new layer and gradually freezing some layers in the network. This work was done on 315 ADNI images and obtained notable accuracy [18].

In the same year, Bit et al. presented an algorithm of combining between Variational Autoencoder (VAE) technology and other machine learning classifiers to classify AD. VAE technology was used to extract low-dimensional featured vectors from MRI images. Machine learning models such as RF, extreme gradient boosting and SVM were exploited for the classification. Data from ADNI and OASIS datasets were utilized. An accuracy of 92% was obtained with this algorithm [19]. To the best of our knowledge, no comprehensive study has established a deep learning network by applying optimization on the CNN architecture specifically for AD levels classification. Thus, this study addresses this by proposing the O-CNN method, in which both CNN architecture and its parameters are optimized. Finally, this work adds a significant contribution in the field of Artificial Intelligence (AI) and it has a further neural network development, which can be used in other studies such as [20][21][22].

3. Methodology

3.1. Proposed O-CNN

In this study, the hybrid O-CNN method is proposed by integrating CNN with Optuna optimization [23].

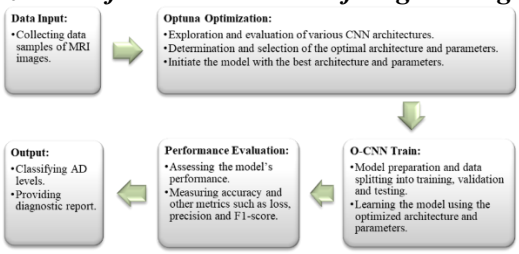

Fig. 2. Main block diagram of the proposed O-CNN approach

Aiming to diagnose and classify AD stages. Specifically, the Optuna optimization is utilized to select the optimal architecture of the CNN network and to efficiently fine-tune its internal parameters. Fig. 2 shows the main block diagram of the proposed O-CNN approach.

Considering the use of two datasets, results in the development of two distinct O-CNN architectures, each tailored to the specific characteristics of its respective dataset. Fig. 3 illustrates the constructed architectures of the two models developed through the utilization of the proposed O-CNN methodology.

In this study, Optuna optimization is employed to enhance the performance of the CNN by judiciously selecting the optimal architecture and meticulously fine-tuning the hyperparameters based on a specific metric. This metric is related to the primary goal that the network aims to reach during the validation accuracy searching process. It can be represented by the following accuracy equation:

$$Accur = \frac{Cop}{Tnp} \times 100\% \qquad (1)$$

where: $Accur$ is the accuracy, Cop is the number of correct predictions and Tnp is the total number of predictions [24][25].

3.2. Optuna optimization

Optuna optimization algorithm is designed to assist tuning the hyperparameters of deep learning [26] networks [27]. It employs an intelligent approach to evaluate and fine-tune a wide range of parameters with the goal of identifying the optimal hyperparameters for the best possible architecture.

Optuna relies on the Tree-structured Parzen Estimator (TPE) for optimizing hyperparameters. TPE is a sophisticated technique that explores and incrementally refines hyperparameters by learning from previous trials [28]. It employs a probabilistic optimization approach, constructing a probabilistic model to differentiate between high-performing and low-performing values, allowing for the intelligent selection of hyperparameters to achieve optimal performance with a minimal number of trials. Fig. 4 displays the workflow of Optuna optimization algorithm.

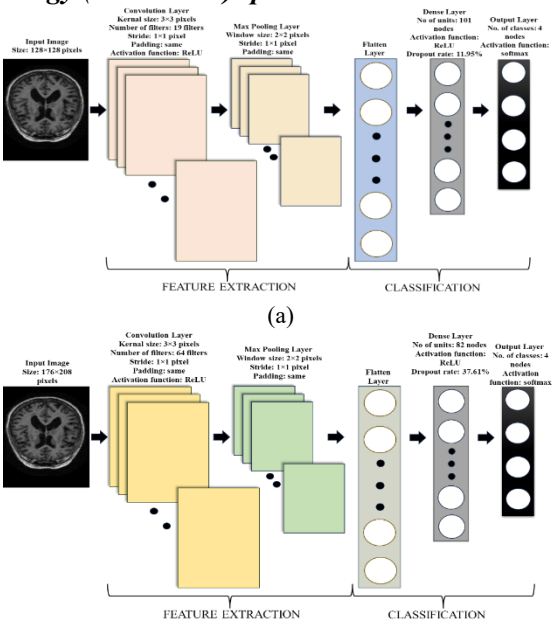

Fig. 3. The constructed architectures and parameters of the two deep learning models using the proposed O-CNN approach, (a) the model for BA-MRI dataset and (b) the model for AD-MRI dataset

The algorithm begins by defining a network with key hyperparameters [29]. These include the number of convolutional layers, number of dense layers, number of filters in the convolutional layers, number of units in the dense layers, learning rate, pooling size, convolutional stride size and dropout rate. These hyperparameters, known as the structural components, they are optimized using Optuna. Optuna works through iterations. During each iteration, it employs the TPE technique to suggest new sets of hyperparameters based on past trials. The models that utilize these hyperparameters are then constructed and trained on a specific dataset. Each model's performance is evaluated based on the validation accuracy, retaining well-performing models and discarding poor ones. This continuous evaluation reduces the number of models per iteration, leading to efficient resource allocation. The process repeats until the best-performing model, with the highest validation accuracy, is identified. Finally, the optimal hyperparameters are used to construct the final model.

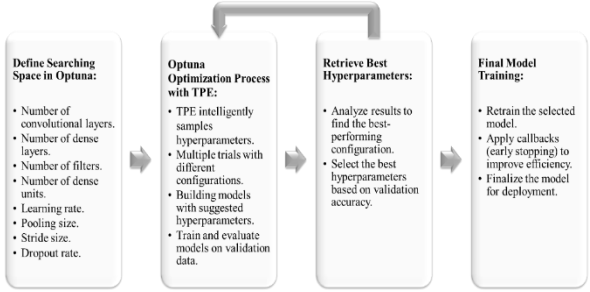

Fig. 4. Representation of the Optuna optimization algorithm workflow

Upon finalizing the optimization process, an integrated model is constructed, reflecting the best configuration of the structural components. The model's exact architecture is customized to deliver the optimal performance on the utilized dataset.

3.3. CNN

CNN is a deep learning type [30] that is specifically made to process data in the form of matrices, such as images [31]. Its architecture is distinguished by its exceptional capability to learn spatial patterns , making it exceptionally valuable at computer vision tasks, such as image classification and segmentation [32].

The architecture of a CNN can be consisted of a number of interconnected layers as the convolutional layer, which is employed to extract key features from the data. This is followed by the Rectified Linear Unit (ReLU) activation function, which introduces non-linearity to the model. In practice, the convolutional layer and ReLU can be considered as a single layer. Subsequently, a max pooling layer is utilized to reduce the dimensionality of the extracted features. Following this is the dropout layer, used to prevent overfitting by randomly setting a fraction of input units to zero during training. The aforementioned layers can be repeated and are all used to extract features from images, the overfitting has been considered in this study, where the validation set is used here to avoid it by early stopping the training implementation. The subsequent layers are responsible for classification. These layers may include a flattening layer, which is used to transform data into one-dimensional vector before feeding it into a dense layer [33]. The dense layer then passes the processed data to the final layer of softmax. In the softmax layer, final decisions are made based on the information received from the fully connected layer [34].

Due to its complex architecture, a CNN can efficiently handle large amounts of data, extracting their patterns and features. This capability is translated into outstanding performance across various domains, especially in tasks as images classification and recognition. Below is the detailed illustration of each layer, along with the mathematical equation which represents its function. The convolutional layer plays a crucial role in extracting various features from an image. The convolution function can be represented by the following equation:

$$H_{\alpha}(a,b) = \sum_{m=1}^{M}\sum_{n=1}^{N} R(m,n) \times W(a-m\,,b-n) \quad (2)$$

Where: H(p,q) represents a calculated convolution value, M and N respectively represents the width and height of the Two-Dimensional (2D) input image, and W(a-m ,b-n) represents a kernel value [35]. It is important to note that the value of H(p,q) is updated for a certain convolution (α) to be H_α (a,b), as numerous convolutional layers may be assembled within the proposed O-CNN.

The activation function can be utilized within the convolutional layer of a CNN, such as ReLU and tanh. The ReLU activation function is widely recognized for preserving positive values and eliminating negative values, thereby introducing non-linearity into the model. This function can be mathematically expressed as follows:

$$Re_{\alpha}(x,y) = max\big(0, H_{\alpha}(a,b)\big) \quad (3)$$

Where: $Re(x,y)$ represents a computed ReLU value and max represents the maximum operation [36]. Also, $Re(x,y)$ is updated for a certain ReLU (α) to be $Re_{\alpha}(x,y)$, as multiple ReLUs can be utilized in the multiple convolutional layers.

Subsequently, the pooling layer reduces the dimensions of the previously analyzed vectors. This layer can be either of type max or average. Max pooling is frequently utilized in CNNs. The general equation for the max pooling can be represented as follows:

$$MP_{\beta}(k,l) = max(\mathbf{S}) \quad (4)$$

Where: $MP(k,l)$ represents a computed pooling value and **S** is a small matrix (or a window) in a previous 2D vector [37]. Similarly, $P(k,l)$ is updated here for a certain pooling layer (β) to be $MP_{\beta}(k,l)$ as also multiple pooling layers can be established in the model.

A flatten layer converts a multi-dimensional vector into a one-dimensional vector [33], preparing the data for the next layer (dense layer). The flatten layer equation can be represented as follows:

$$Fla[i] = \sum_{g=1}^{h}\sum_{f=1}^{w}\sum_{r=1}^{e} T[g][f][r] \quad (5)$$

where: $Fla[i]$ represents the flattened output for the ith sample, $T[g][f][r]$ refers to a value in a Three-Dimensional (3D) matrix, and h, w and e are the numbers of rows, columns and channels, respectively. This layer encapsulates extracted features of the previous layer, where they are transformed into One-Dimensional (1D) vector suitable for processing in the next layer [38].

Dense layer (or fully connected layer) connects each neuron in the previous layer to all neurons in its layer.

Table 1. Comparisons between the BA-MRI and AD-MRI datasets.

Specification	BA-MRI	AD-MRI
Source	Original and synthetic axial MRI scans	Axial MRI scans
MRI Scanner Strength	1.5 Tesla	---
Sequence	T1-weighted	---
Image Resolution	128 × 128 pixels	208 × 176 pixels
Preprocessing	Skull removal	---
Total No. of Images	11,519	2,609
No. of MD Images	2,739	646
No. of MoD Images	2,572	637
No. of ND Images	3,200	652
No. of VMD Images	3,008	674

The fundamental equation describing the fully connected layer can be expressed as follows:

$$DE_{\gamma}(c) = B(c) + \sum_{z=1}^{b} \left(FW(c,z) \times N(z) \right) \quad (6)$$

where: $DE(c)$ represents an output value of the dense layer, c represents the number of units (nodes) in the fully connected layer, $B(c)$ represents a bias value, b represents the number of units in the previous layer, $FW(c,z)$ represents a connection weight value between the pooling and fully connected layers, and $N(z)$ represents the output value of a node in the previous layer [39]. Likewise, $DE(c)$ is updated in this study for a certain pooling layer (γ) to be $DE_{\gamma}(c)$ as multiple dense layers can be provided in the model too.

The output layer is ultimately employed for the specified classification task. Fundamentally, this layer utilizes the softmax activation function. The core equation for this function can be expressed as follows:

$$SoMx(C) = \frac{e^{DE_{\gamma}(c)}}{\sum_{lo=1}^{K} e^{DE_{\gamma}(lo)}} \quad (7)$$

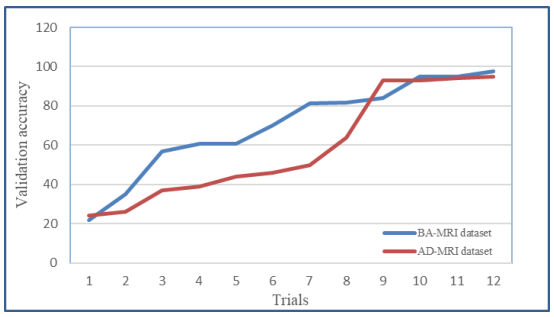

Fig. 1. Effectiveness of validation during implementing the O-CNNs for both datasets

Where: $SoMx(C)$ represents a calculated softmax value for class C and K is the number of classes [40][41].

Table 2. Establishment of O-CNN Model for AD-MRI dataset.

Layer Type	Kernal Size (pixels/nodes)	No. of Filters	Output Shape (pixels/nodes)	No. of Trainable Parameters
Convolution layer 1	3×3	64	176×208×64	640
Max pooling layer 1	2×2	---	88×104×64	0
Flatten layer	---	---	585728	0
Dense layer 1	82	---	82	48029778
Dropout layer 1	82	---	82	0
Dense layer 2	4	---	4	332
Total no. of parameters				144092252
No. of trainable parameters				48030750
No. of non-trainable parameters				0
No. of optimizer params				96061502

4. Results and Discussion

4.1. Utilized Datasets

Two MRI image datasets are utilized in this study, called the BA-MRI [42] and AD-MRI [43]. Both datasets encompass brain MRI images reviewed and examined by medical experts. Each image is of Joint Photographic Experts Group (JPG) format. The MRI images within each dataset are divided into four AD levels: Mild Dementia (MD), Moderate Dementia (MoD), Non-Dementia (ND) and Very Mild Dementia (VMD). This categorization has been utilized for the classification purpose in this work. For better clarity, **Table 1** displays comparisons between the BA-MRI and AD-MRI datasets.

BA-MRI dataset comprises of a combination of original and synthetic axial MRI scans. The scans were obtained using 1.5 Tesla MRI scanner with a T1-weighted sequence. Each image has the resolution of 128×128 pixels. All images underwent preprocessing to remove skulls in the sourced dataset. In total, this dataset consists of 11,519 images, 2739 images for MD, 2572 images for MoD, 3200 images for ND and 3008 images for VMD. AD-MRI dataset consists of images captured using a Magnetic Resonance Imaging (MRI) scanner. Each is of the resolution 208 × 176 pixels.

Table 2. Establishment of O-CNN Model for BA-MRI dataset.

Layer Type	Kernal Size (pixels/nodes)	No. of Filters	Output Shape (pixels/nodes)	No. of Trainable Parameters
Convolution Layer 1	3×3	19	128×128×19	190
Max Pooling Layer 1	2×2	---	64×64×19	0
Flatten Layer	---	---	77824	0
Dense Layer 1	101	---	101	7860325
Dropout layer 1	101	---	101	0
Dense Layer 2	4	---	4	408
Total no. of parameters				23582771
No. of trainable parameters				7860923
No. of non-trainable parameters				0
No. of optimizer params				15721484

In total, 2609 images are contained in this dataset. They are divided as the following categories: 646 images for MD, 637 images for MoD, 652 images for ND and 674 images for VMD. This dataset was unprocessed. Actually, this can be appropriate opportunity to investigate the flexibility of the proposed approach to handle data without preparations. It was also obtained from Kaggle, as mentioned.

4.2. Experimental setup

Firstly, all experiments were conducted using a laptop with the following specifications: a Lenovo model, Intel Core™ i7 processor of the 5th generation, operating at speed 2.4 GHz, 8 GB Random Access Memory (RAM), and external NVIDIA GeForce graphics card with 4 GB memory. The Google Colab environment was also utilized for processing the two datasets which employed in this study. Initially, each dataset was divided into three distinct subsets for training, testing and validation, with the proportions of 70%, 15% and 15%, respectively.

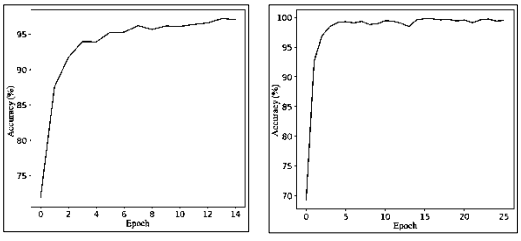

(a) (b)

Fig. 2. Training accuracy curves (a) for AD-MRI dataset and (b) for BA-MRI dataset.

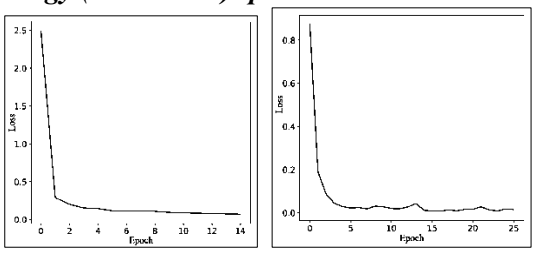

(a) (b)

Fig. 7. Training Loss (error) curves (a) for AD-MRI dataset and (b) for BA-MRI dataset.

4.3. O-CNN results and discussion

The architecture of the suggested O-CNN model, which is especially designed for the used dataset is dynamically optimized to obtain its number of convolutional layers, number of dense layers, number of filters, number of dense units, learning rate, pooling size, convolutional stride size and dropout rate. O-CNN performs the experiments and evaluates the validation accuracy for each trial. Fig. 1 shows the Effectiveness of validation during implementing the O-CNNs for both datasets.

After the O-CNN experiments are finished, the best model is kept. **Error! Reference source not found.Error! Reference source not found.** and Table 2 provide an overview of the final architectural configuration of O-CNN models for both datasets.

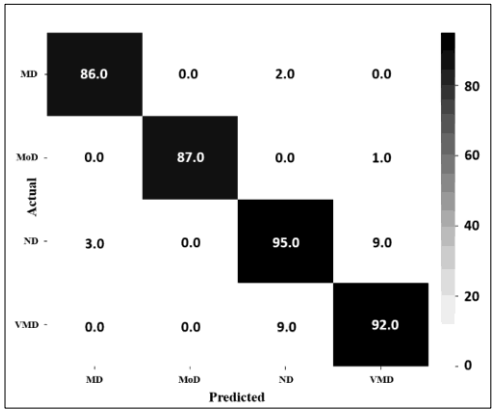

(a)

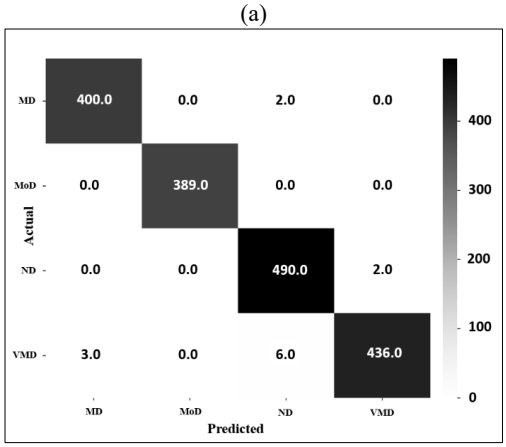

(b)

Fig. 3. Confusion matrices of testing the O-CNN models (a) for AD-MRI dataset and (b) for BA-MRI datasets

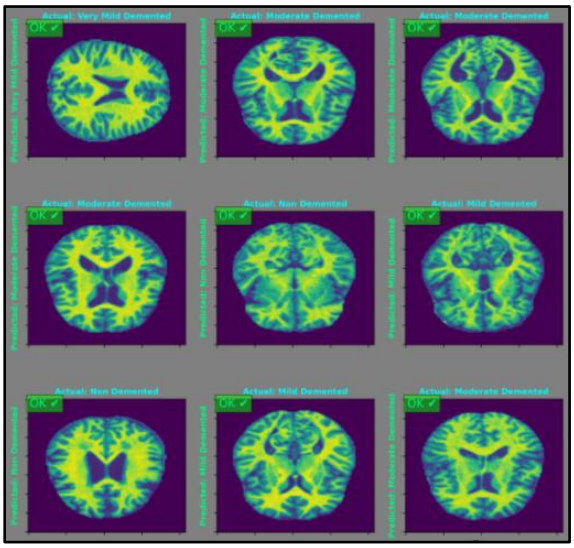

(a)

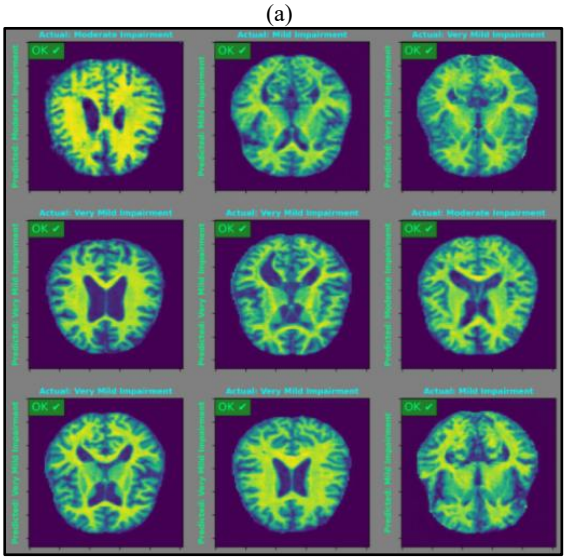

(b)

Fig. 4. Prediction examples of the O-CNN models (a) for AD-MRI dataset and (b) for BA-MRI datasets.

All of the parameters that were established following the use of Optuna optimization are also included in both tables, which aid in creating the best possible architectures for the suggested OCNN models.

Subsequently, the O-CNN models are trained using the training sets and monitored via the validation sets. Remarkable outcomes and high training accuracies are attained for both datasets, with a training accuracy equals to 99.47% for BA-MRI and equals to 97.09% for AD-MRI. Fig. 6 illustrates the training accuracy curves for both datasets under consideration. Fig. 7 depicts the training loss (error) curves for the utilized datasets.

The model's validation accuracy after training is 99.53% for the BA-MRI dataset and 95.57% for the AD-MRI dataset. These outcomes demonstrate how well the O-CNN models performed during the validation stage.

The confusion matrix, which assists in calculating the proportion of properly and erroneously identified examples for each class, is one of the most often used techniques for assessing testing accuracy. The confusion matrices of testing the O-CNN models for both used datasets are displayed in Fig. 8, which illustrates the connections between the actual and predicted cases for each class. The testing accuracies of the proposed models are recorded as 99.18% for the BA-MRI dataset and 95.79% for the AD-MRI dataset.

The predictive power and performance of the O-CNN models in classifying AD into various levels are illustrated in Fig. 9. The ability of each model in categorizing AD levels is demonstrated by the visual comparisons between actual and predicted classes. Our suggested O-CNN combines CNN and Optuna optimization to deliver the best-established architecture with parameters, as is one of its many distinctive features.

It has also been evaluated on two MRI datasets and demonstrated noteworthy outcomes in predicting the phases of AD, making it a trustworthy tool to help clinicians with their diagnosis. Optuna can outperform conventional optimization frameworks such as Bayesian optimization and grid search by utilizing its adaptive Tree-structured Parzen Estimator (TPE). It also has the ability to provide parallel execution. Furthermore, it can be quickly implemented for tuning hypermeters and obtaining the optimal architecture of CNN. All of these make Optuna exceptionally effective compared to other methods.

5. Conclusion

A hybrid strategy was considered in this study, where an efficient optimization was exploited to configure a deep learning network. CNN and Optuna optimization were effectively combined to provide an O-CNN architecture. The aim of this integration is to generate a CNN architecture by adjusting its settings using Optuna optimization. This approach aims to classify four AD stages or levels (MD, MoD, ND and VMD) from MRI brain images. The latest O-CNN model is used to guarantee the best fit for the dataset.

The proposed technique was rigorously tested on two distinct datasets, resulting in notably high classification accuracies. The O-CNN model for the BA-MRI dataset exhibited exceptional performance, achieving the training accuracy of 99.47%, validation accuracy of 99.53% and testing accuracy of 99.18%. Similarly, the O-CNN model for the AD-MRI dataset demonstrated remarkable results, attaining the training accuracy of 97.09%, validation accuracy of 95.57% and testing accuracy

of 94.79%. This makes our proposed models trustworthy in helping clinicians with AD diagnosis. In future, a massage can be presented to clinician to make decision as they can early recognize and treat AD patients. By concentrating on the early to intermediate dragonize, doctors may select the best therapies for patients.

References

[1] Murtala Bello Abubakar, Kamaldeen Olalekan Sanusi, Azizah Ugusman, Wael Mohamed, Haziq Kamal, Nurul Husna Ibrahim, Ching Soong Khoo and Jaya Kumar, "Alzheimer's Disease: An Update and Insights Into Pathophysiology," Frontiers in Aging Neuroscience, vol. 14, no. Article 742408, pp. 1–16, 2022, doi: 10.3389/fnagi.2022.742408.

[2] Chih-Sung Liang, Dian-Jeng Li, Fu-Chi Yang, Ping-Tao Tseng, Andre F Carvalho, Brendon Stubbs, Trevor Thompson, Christoph Mueller, Jae Il Shin, Joaquim Radua, Robert Stewart, Tarek K Rajji, Yu-Kang Tu, Tien-Yu Chen, Ta-Chuan Yeh, Chia-Kuang Tsai and Chia-L, "Mortality rates in Alzheimer's disease and non-Alzheimer's dementias: a systematic review and meta-analysis," The Lancet Healthy Longevity, vol. 2, no. 8, pp. e479–e488, 2021, doi: 10.1016/S2666-7568(21)00140-9.

[3] Marina Ávila-Villanueva, Alberto Marcos Dolado, Jaime Gómez-Ramírez and Miguel Fernández-Blázquez, "Brain Structural and Functional Changes in Cognitive Impairment Due to Alzheimer's Disease," Frontiers in Psychology, vol. 13, pp. 1–6, 2022, doi: 10.3389/fpsyg.2022.886619.

[4] Samantha McGirr, Courtney Venegas and Arun Swaminathan, "Alzheimer ' s Disease : A Brief Review," Journal of Experimental Neurology, vol. 1, no. 3, pp. 89–98, 2020.

[5] Koji Hori, Kimiko Konishi, Masayuki Tani, Hiroi Tomioka, Ryo Akita, Yuka Kitajima, Mari Aoki, Nodoka Kikuchi, Daisuke Ikuse, Norihisa Akashi, Misa Hosoi, Koichi Jimbo and Mitsugu Hachisu, "Antidemenia Agents are Partially Symptomatic Treatment and Partially Disease Modifying Treatment," Brain Disorders & Therapy, vol. 04, no. 01, 2015, doi: 10.4172/2168-975x.1000148.

[6] Martha Storandt, Elizabeth Grant, J. Philip Miller and John Morris, "Rates of progression in mild cognitive impairment and early Alzheimer's disease," Neurology, vol. 59, no. 7, pp. 1034–1041, 2002, doi: 10.1212/WNL.59.7.1034.

[7] Rebecca G. Logsdon, Laura E. Gibbons, Susan M. McCurry and Linda Teri, "Quality of Life in Alzheimer's Disease Caregiver," Journal of Mental and Aging, vol. 5, 1999.

[8] Stephanie Johanna Beatrix Vos, Ineke Anna van Rossum, Frans Verhey, Dirk Lodewijk Knol, Hilkka Soininen, Lars-Olof Wahlund, Harald Hampel, Magda Tsolaki, Lennart Minthon, Giovanni Battista Frisoni, Lutz Froelich, Flavio Nobili, Wiesje van der Flier and Ka, "Prediction of Alzheimer disease in subjects with amnestic and nonamnestic MCI," Neurology, vol. 80, no. 12, pp. 1124–1132, 2013, doi: 10.1212/WNL.0b013e318288690c.

[9] Giulia Fiscon, Emanuel Weitschek, Giovanni Felici, Paola Bertolazzi, Simona De Salvo, Placido Bramanti and Maria Cristina De Cola, "Alzheimer's disease patients classification through EEG signals processing," Symposium on Computational Intelligence and Data Mining, Proceeding, pp. 105–112, 2014, doi: 10.1109/CIDM.2014.7008655.

[10] Hamed Taheri Gorji and Javad Haddadnia, "A novel method for early diagnosis of Alzheimer's disease based on pseudo Zernike moment from structural MRI," Neuroscience, vol. 305, pp. 361–371, 2015, doi: 10.1016/j.neuroscience.2015.08.013.

[11] Debesh Jha and Goo-Rak Kwon, "Alzheimer Disease Detection in MRI Using Curvelet Transform with K-NN," Journal of Korean Institute of Information Technology, vol. 14, no. 8, pp. 121–129, 2016, doi: 10.14801/jkiit.2016.14.8.121.

[12] Kajal Kiran Gulhare, Soorya Prakash Shukla and Lokesh Kumar Sharma, "Deep Neural Network Classification method to Alzheimer's Disease Detection," International Journals of Advanced Research in Computer Science and Software Engineering, vol. 7, no. 6, 2017, doi: 10.13140/RG.2.2.31207.75687.

[13] Alexander Khvostikov, Karim Aderghal, Jenny Benois-Pineau, Andrey Krylov and Gwenaelle Catheline, "3D CNN-based classification using sMRI and MD-DTI images for Alzheimer disease studies," arXiv:1801.05968v1, vol. 1, 2018, doi: 10.1016/j.neuroimage.2018.01.070.

[14] Muazzam Maqsood, Faria Nazir, Umair Khan, Farhan Aadil and Habibullah Jamal, "Transfer Learning Assisted Classification and Detection of Alzheimer's Disease Stages Using 3D MRI Scans," Sensors, vol. 19, no. 12, p. 2645, 2019, doi: 10.3390/s19112645.

[15] Akash Rajak and Ajay Kumar Shrivastava, "Diagnosis of Alzheimer Disease using Machine Learning Approaches," International Journal of Advanced Science and Technology, vol. 29, no. 04, pp. 7062–7073, 2020, [Online]. Available: https://www.researchgate.net/publication/342847161

[16] Xiaowang Bi, Wei Liu, Huaiqin Liu and Qun Shang, "Artificial Intelligence-basedMRIImages for Brain in Prediction of Alzheimer's Disease," Journal of Healthcare Engineering, 2021, doi: 10.1155/2021/8198552.

[17] Jinhua Sheng, Yu Xin, Qiao Zhang, Luyun Wang, Ze Yang and Jie Yin, "Predictive classification of Alzheimer's disease using brain imaging and genetic data," Scientific Reports, vol. 12, no. 1, p. 2405, 2022, doi: 10.1038/s41598-022-06444-9.

[18] Rizwan Khan, Saeed Akbar, Atif Mehmood, Farah Shahid, Khushboo Munir, Naveed Ilyas, Muhammad Asif and Zhonglong Zheng, "A transfer learning approach for multiclass classification of Alzheimer's disease using MRI images," Frontiers in Neuroscience, vol. 16, p. 1050777, 2023, doi: 10.3389/fnins.2022.1050777.

[19] Subhrangshu Bit, Pritam Dey, Arnab Maji and Tapan K Khan, "MRI-based mild cognitive impairment and Alzheimer's disease classification using an algorithm of combination of variational autoencoder and other machine learning classifier," Journal of Alzheimer's Disease Reports, vol. 8, pp. 1093–1111, 2024, doi: 10.1177/25424823241290694.

[20] Adnan A.Ismael, Abdulnaser A.Ahmed, Raid Rafi Omar Al-Nima, and Mohammed Khaire Hussain, "Prediction of the drainage coefficient of steeply crested inclined weirs using different neural network techniques," NTU Journal of Engineering and Technology, vol. 2, no. 4, pp. 41–44, 2023.

[21] Raid Rafi Omar Al-Nima, Lubab H.Albak and Arwa H.Al-Hamdany, "Translating Sumerian Symbols into French Letters," NTU Journal of Engineering and Technology, vol. 3, no. 1, pp. 12–17, 2024.

[22] Duaa Mowafak Hameed and Raid Rafi Omar Al-Nima, "High-Performance Character Recognition System Utilizing Deep Convolutional Neural Networks," NTU Journal of Engineering and Technology, vol. 3, no. 4, pp. 42–51, 2024.

[23] Sadaqat ur Rehman, Shanshan Tu, Obaid ur Rehman, Yongfeng Huang, Chathura M. Sarathchandra Magurawalage and Chin-Chen Chang, "Optimization of CNN through novel training strategy for visual classification problems," Entropy, vol. 20, no. 4, pp. 1–10, 2018, doi: 10.3390/e20040290.

[24] Marina Sokolova, Nathalie Japkowicz and Stan Szpakowicz, "Beyond Accuracy, F-score and ROC: a Family of Discriminant Measures for Performance Evaluation," Advances in Artificial Intelligence, pp. 1015–1021, 2006.

[25] Hossam Magdy Balaha, Hesham Arafat Ali, Mohamed Saraya and Mahmoud Badawy, "A new Arabic handwritten character recognition deep learning system (AHCR-DLS)," Neural Computing and Applications, vol. 33, no. 11, pp. 6325–6367, 2021, doi: 10.1007/s00521-020-05397-2.

[26] Raid Rafi Omar Al-Nima, Saba Qasim Hasan, and Sahar Esmaiel Mahmood, "Utilizing Fingerphotos with Deep Learning Techniques to Recognize Individuals," NTU Journal of Engineering and Technology, vol. 2, no. 1, pp. 39–45, 2023.

[27] Jenia Afrin Jeba, "Case study of Hyperparameter optimization framework Optuna on a Multi-column Convolutional Neural Network," 2021.

[28] Yoshihiko Ozaki, Yuki Tanigaki, Shuhei Watanabe, Masahiro Nomura and Masaki Onishi, "Multiobjective Tree-Structured Parzen Estimator," Journal of Artificial Intelligence Research, vol. 73, pp. 1209–1250, 2022, doi: 10.1613/jair.1.13188.

[29] Rana Ahmed Lateef and Ayad Razi Abbas, "Tuning the Hyperparameters of the 1D CNN Model to Improve the Performance of Human Activity Recognition," Engineering and Technology Journal, vol. 40, no. 4, pp. 547–554, 2022, doi: 10.30684/etj.v40i4.2054.

[30] Silvia Basaiaa, Federica Agostaa, Luca Wagnerc, Elisa Canua, Giuseppe Magnanib, Roberto Santangelob and Massimo Filippia, "Automated classification of Alzheimer's disease and mild cognitive impairment using a single MRI and deep neural networks," NeuroImage: Clinical, vol. 21, p. 101645, 2019, doi: 10.1016/j.nicl.2018.101645.

[31] Bijen Khagi, Chung Ghiu Lee and Goo-Rak Kwon, "Alzheimer's disease classification from brain MRI based on transfer learning from CNN," in biomedical engineering international conference (BMEiCON), IEEE, 2018.

[32] Mahbub Hussain, Jordan James Bird and Faria Diego Ricardo, "A Study on CNN Transfer Learning for Image Classificatio," Advances in Intelligent Systems and Computing, vol. 840, pp. 191–202, 2019, doi: 10.1007/978-3-319-97982-3_16.

[33] Alex Krizhevsky, Ilya Sutskever and Geoffrey E. Hinton, "Neural Networks," Encyclopedia of Movement Disorders, Three-Volume Set, vol. 3, pp. V2-257-V2-259, 2010, doi: 10.1016/B978-0-12-374105-9.00493-7.

[34] Laith Alzubaidi, Juan Santamaría, Mohammed Ali Fadhel, Muthana Al-Amidie, Laith Farhan, Jinglan Zhang, Amjad J. Humaidi, Ayad Al-Dujaili, Ye Duan and Omran Al-Shamma, "Review of deep learning: concepts, CNN architectures, challenges, applications, future directions," Journal of Big Data, vol. 8, no. 1, 2021, doi: 10.1186/s40537-021-00444-8.

[35] Saad Albawi, Tareq Abed Mohammed and Saad AL-Zawi, "Understanding of a Convolutional Neural Network," Proceedings of 2017 International Conference on Engineering and Technology, ICET 2017, pp. 1–6, 2017, doi: 10.1109/ICEngTechnol.2017.8308186.

[36] Ahmed Saeed Ibrahim Al-Obaidi, Raid Rafi Omar Al-Nima, and Tingting Han, "Interpreting Arabic Sign Alphabet by Using the Deep Learning," AIP Conference Proceedings, vol. 2862, no. 1, pp. 29–30, 2023, doi: 10.1063/5.0171428.

[37] Ihsan Evanjelist Firdausi, Irfan Mukhlash, Atyah Dhamar Syah Gama and Naufal Hidayat, "Sentiment analysis of customer response of telecommunication operator in Twitter using DCNN-SVM Algorithm," Journal of Physics: Conference Series, vol. 1490, no. 1, 2020, doi: 10.1088/1742-6596/1490/1/012071.

[38] Ernest Jeczmionek and Piotr Adam Kowalski, "Flattening layer pruning in convolutional neural networks," Symmetry, vol. 13, no. 7, pp. 1–13, 2021, doi: 10.3390/sym13071147.

[39] Wu Hao and Zhao Jinsong, "Deep convolutional neural network model based chemical process fault diagnosis," Computers & chemical engineering, vol. 115, pp. 185–197, 2018.

[40] Sagheer Abbas , Yousef Alhwaiti , Areej Fatima , Muhammad A. Khan , Muhammad Adnan Khan, Taher M. Ghazal, Asma Kanwal, Munir Ahmad and Nouh Sabri Elmitwally, "Convolutional neural network based intelligent handwritten document recognition," Computers, Materials and Continua, vol. 70, no. 3, pp. 4563–4581, 2022, doi: 10.32604/cmc.2022.021102.

[41] Weiyang Liu, Yandong Wen, Zhiding Yu and Meng Yang, "Large-Margin Softmax Loss for Convolutional Neural Networks," Proceedings of the 33rd International Conference on Machine Learning, vol. 48, 2016, [Online]. Available: http://arxiv.org/abs/1612.02295

[42] Kaggle, "Best Alzheimer MRI dataset," Accessed September 30, 2024, 2024, [Online]. Available: https://www.kaggle.com/datasets/lukechugh/best-alzheimer-mri-dataset-99-accuracy

[43] Kaggle, "Alzheimers disease MRI images," Accessed September 30, 2024, 2024, [Online]. Available: https://www.kaggle.com/datasets/shariaarfin/alzheimers-disease-mri-images?resource=download